

1 **REWARE: A seismic processing algorithm to retrieve geological information**
2 **from the water-column**

3

4 Romain SYLVAIN¹, Louise WATREMEZ¹, Isabelle THINON², Frank CHANIER¹, Fabien
5 CAROIR^{1,3}, Virginie GAULLIER¹

6 ¹ Univ. Lille, CNRS, Univ. Littoral Côte d'Opale, IRD, UMR 8187, LOG, Laboratoire
7 d'Océanologie et de Géosciences, 59000 Lille, France

8 ² BRGM (Bureau de Recherches Géologiques et Minières), 45060 Orléans, France

9 ³ Sorbonne Université, CNRS-INSU, Institut des Sciences de la Terre de Paris ISTeP,
10 F75005 Paris, France

11

12

13 Romain SYLVAIN (corresponding author): romain.sylvain@univ-lille.fr

14 Louise WATREMEZ: louise.watremez@univ-lille.fr

15 Frank CHANIER: frank.chanier@univ-lille.fr

16 Virginie GAULLIER: virginie.gauillier@univ-lille.fr

17 Isabelle THINON: i.thinon@brgm.fr

18 Fabien CAROIR: fabien.caroir@sorbonne-universite.fr

19

20

21

22

23 **Abstract**

24 When interpreting marine Very High-Resolution (VHR) single-channel seismic reflection data,
25 the signal in the water-column is generally considered as noise and is often eliminated by a
26 water-mute application to focus on geological information under the seafloor. Alternatively,
27 the signal in the water-column can be used to study ocean currents or gas/fluid emissions.
28 To provide images of the sedimentary formations and tectonic structures beneath the
29 seafloor in shallow water regions, such as continental shelves and lakes, marine seismic
30 reflection profiles are often acquired using a single-channel streamer and sparker-type
31 source, providing VHR data, with limited penetration-depth. To exploit the full potential of
32 these single-channel data, we propose a simple algorithm, called REWARE (Recovery of
33 Water-column Acoustic Reflectors). This algorithm allows to extract further geological
34 information from the water-column data using open-source codes (Seismic Un*x), adding the
35 coherent signal from the previous shots, recorded in the water-column, to the previous
36 traces. The record length becomes longer while maintaining a very high trace-to-trace
37 consistency. To demonstrate its efficiency, we present two examples of the REWARE
38 processing in two different geological contexts: the East Sardinia shelf (Italy) and the North
39 Evia Gulf (Greece). This method provides deeper images than with original data for seismic
40 data acquired across steep slopes, such as canyons or continental shelf breaks. Thus,
41 depending on the seafloor geometry and sub-seafloor structures, it is possible to image or
42 map sediment layers and tectonic structures at depth, keeping a very high structural
43 resolution.

44 Keywords: Geophysical Methods; Seismic Noise; Seismic Instruments; Image Processing

45 1. Introduction

46 Continental shelves and shallow water basins can be the locus of various sedimentary and
47 tectonic processes leading to the development of complex organisations of sedimentary
48 bodies and/or faulting and folding. Very High-Resolution (VHR) seismic reflection is widely
49 used for shallow water-depth investigations (<1000 m) to image these geological features.
50 The source used is generally a sparker combined with a single or multi-channel streamer.
51 The processing of multi-channel seismic data is widely detailed in the literature and several
52 dedicated softwares exist (e.g. Yilmaz & Doherty 2001; Dondurur 2018; Kluesner *et al.*
53 2019). However single-channel processing is sometimes underestimated but is as essential
54 as the processing of multi-channel seismic data (Santos *et al.* 2021). Several authors have
55 recently suggested (1) processing tools for single-channel data to improve the resolution of
56 sparker seismic data, (2) new strategies of waveform analysis for deconvolution and random
57 noise reduction, and also (3) complete processing workflows (e.g. Duchesne *et al.* 2007;
58 Kluesner *et al.* 2019; Jun *et al.* 2020; Santos *et al.* 2021). These processing methods do not
59 account for the signal in the water-column. This signal is commonly used for oceanographic
60 studies (e.g. Bakhtiari Rad & Macelloni 2020), current analysis, water temperature gradients
61 (e.g. Ruddick *et al.* 2009) or gas and oil leaks. For sub-seafloor studies, the water-column
62 data is generally ignored. However, the water-column data contains coherent signal,
63 considered as “noise” from the previous shot, which contains actual geological information.
64 This information can be extracted to extend the trace length and observe geological features
65 at greater depth than from the original data and typical processing.

66 The selection of acquisition parameters, such as record length, shot spacing and seismic
67 energy output, for VHR single-channel seismic reflection data at shallow water depths can be
68 challenging in the light of the quest for optimal seismic penetration depth and the
69 complications due to bathymetric variations. For example, assuming acquisition parameters
70 set for a water-column of 50 to 100 m (sea-bottom is reached at 66 ms and its multiple at
71 132 ms) and a study area characterised by strong bathymetry variations (e.g. canyon heads

72 or shelfbreak zones), the record time can be locally too short to record signal in the
73 geological layers. An increase of the record length and shot interval would degrade the
74 lateral trace-to-trace consistency of the data, i.e. the lateral continuity of the geological
75 signal. The objective here is to retrieve and use the coherent reflections from previous shots
76 in the water-column in order to obtain geological information at greater depth than from the
77 originally acquired data.

78 We developed a processing algorithm called REWARE (Recovery of Water-column Acoustic
79 Reflectors), using tools from Seismic Un*x (Stockwell 1999; Cohen & Stockwell 2021) to
80 retrieve the geological reflectors from the water-column data. This algorithm artificially
81 increases the recording length, duplicating the data. It extracts the signal recorded in the
82 water-column of a seismic trace to add it after the previous trace to create a new seismic
83 image down to greater depth than from the raw data. We tested this workflow on marine VHR
84 seismic profiles from two examples: the East Sardinia shelf (Western Tyrrhenian Sea, Italy),
85 dissected by deep canyons with a highly variable bathymetry (50–1000 m); and the North
86 Evia rift basin (NW Aegean Sea, Greece), a sedimentary basin in a tectonically active
87 system.

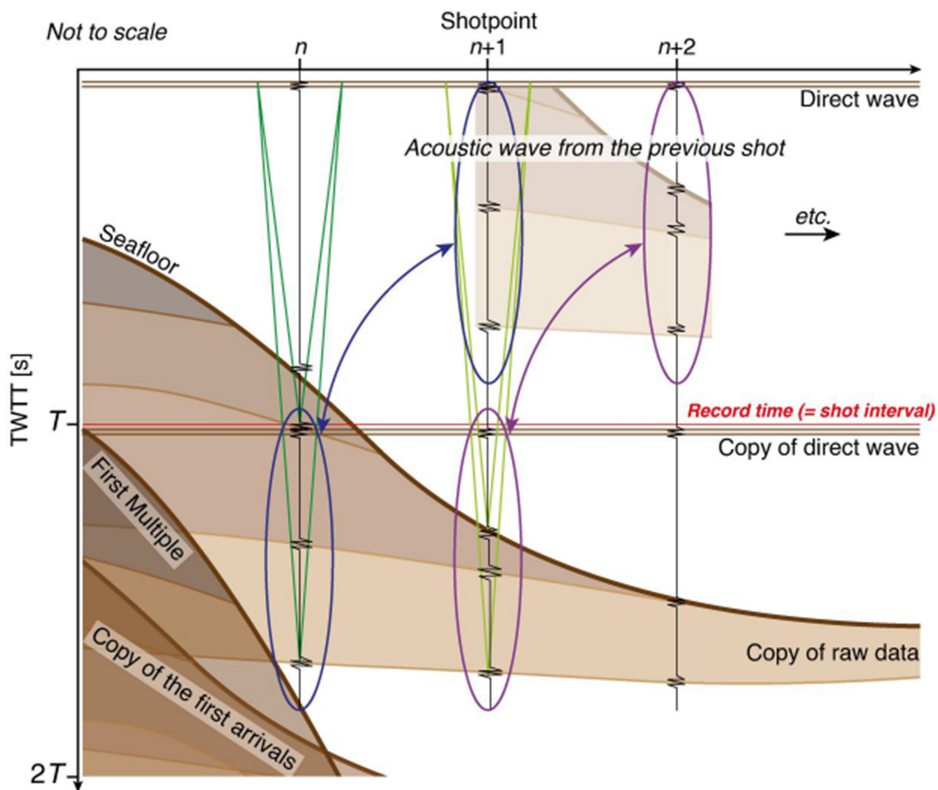
88

89 **2. REWARE: Principle**

90 The resolution of the data mainly depends on the frequency band of the seismic source
91 (Yilmaz & Doherty 2001). In particular, the vertical resolution is controlled by the signal
92 frequency whereas the lateral resolution mostly depends on the width of the Fresnel zone,
93 which is related to the signal frequency, but also the depth to the considered reflector and
94 seismic velocities. Vertical resolution may be improved using deconvolution and 2D migration
95 helps improve lateral resolution (Yilmaz & Doherty 2001). Finer trace spacing increases
96 trace-by-trace consistency (Dondurur 2018). In shallow water areas, it is important to record
97 data with an optimal resolution and fine trace spacing. The shot interval dictates the record

98 length, and thus the maximum depth of recorded reflections. When the bathymetry of the
 99 study area is variable, the record time can be too short in some places, and the signal of
 100 interest is cut by the end of the trace. In deep bathymetry areas, only the water-column may
 101 be recorded on the seismic trace (Fig 1, down to time T). Variable bathymetry requires
 102 frequent changes in acquisition parameters leading to acquisition gaps, or the need to loop
 103 back during the survey, which is time-consuming. An alternative would be to set a longer
 104 shot interval to increase the signal penetration. However, an increase of investigation depth
 105 is usually associated with an increase of the source energy used – and thus the signal
 106 frequencies – and shot spacing. The expected vertical and lateral resolutions (lower
 107 frequency signal and trace-to-trace consistency) would be degraded.

108



109

110 Figure 1. Diagram of the ray paths at increasing water depths illustrating the occurrence of

111 reflections from previous shots, recorded in the water-column, for short shot interval and

112 *record time of Very-High-Resolution seismic data. The record time is equal to the shot*
113 *interval.*

114

115 When acquiring data of shots at a constant time interval, it is possible to set the record length
116 equal to this shot time interval (T). With this acquisition parameter, the late arrivals from a
117 shot n may still be recorded on the trace of shot $n+1$ (Fig. 1). The useful observation of
118 geological reflections from the previous shot in the water layer implies a sufficiently deep
119 seafloor, which also avoids a too early multiple reflection, overlapping reflections of interest.

120 We consider a seismic section with N seismic traces, and a record length equal to the shot
121 interval (T). The purpose is to extract the signal recorded in the water-column of traces 2 to
122 N . This signal belongs to the traces 1 to $N-1$, at times of T to $2T$.

123

124 **3. Processing algorithm**

125 The REWARE processing algorithm uses the open-source package Seismic Un*x (Stockwell
126 1999; Cohen & Stockwell 2021). Shell scripts and further details about the procedure are
127 presented in Supplementary Material A.

128 We consider a seismic section with N seismic traces and a raw record length, T , in Two Way
129 Travel-Time (TWTT, Fig. 2a). The coherent signal, in the water-column of a trace $n+1$
130 between the sea-level ($t = 0$) and the seafloor reflector, corresponds to late arrivals from the
131 previous shot (trace n). The operation consists in adding the data of trace $n+1$ at the end of
132 trace n , starting from the record time T , and obtain a trace n with an extended record length
133 of $2T$.

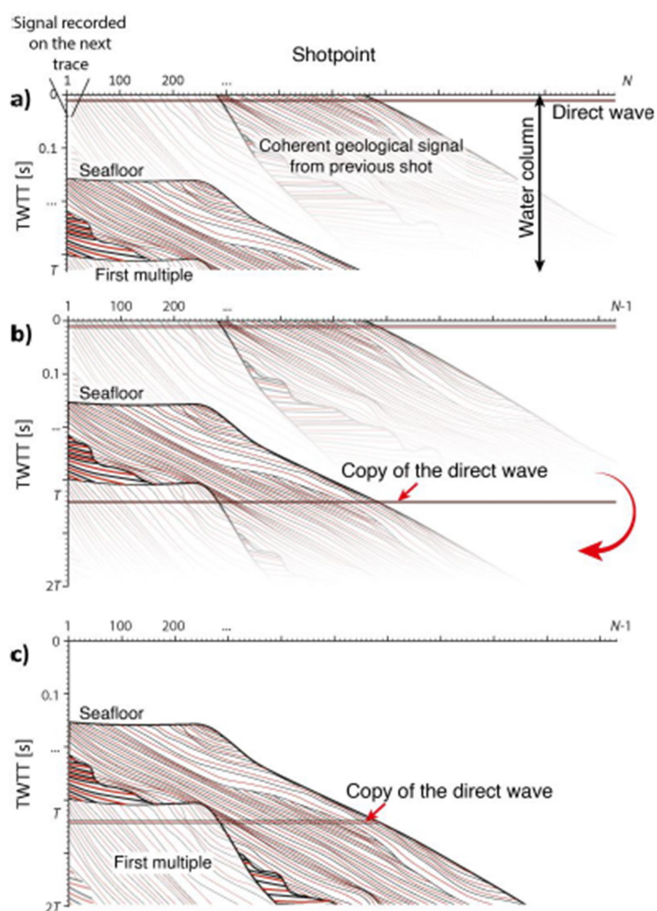
134 The algorithm comprises two steps (Fig. 2):

- 135 1) Extract two copies of the data: the first with traces 1 to $N-1$ extracted (D1), and the
136 second with traces 2 to N (D2) (Fig. 2a);

137 2) Merge both datasets D1 and D2 by concatenation of D2 after D1, in time (Fig. 2b).
 138 We obtain an updated seismic section with an extended record length, called SD.
 139 Note that a copy of the direct wave appears in the middle of the SD seismic profile.

140

141 The conditions to use REWARE are (1) a bathymetry allowing for the observations of
 142 coherent geological reflections from the previous shot above the seafloor reflector, and (2)
 143 equal record length and shot interval. Meeting this condition is mandatory to receive the late
 144 arrivals directly on a trace $n+1$. Existing public datasets also check those conditions (for
 145 example, see profiles HC-12; SB-102 and SB-143 in Sliter *et al.* (2008)



146

147 Figure 2. Sketches of the REWARE algorithm: (a) raw data (b) Merging of D1 and D2 (c)
 148 Resulting seismic section after muting of water-column information.

148

150 **4. Application on two examples**

151 The seismic processing workflow, incorporating the REWARE algorithm, applied to marine
152 VHR single-channel seismic data, enables the utilisation of signals typically regarded as
153 noise in the water-column. This workflow reduces the need for changing the acquisition
154 parameters (shot interval, vessel speed, record length) during the acquisition surveys, when
155 bathymetry varies rapidly, keeping a high trace-to-trace consistency, even in deeper areas.

156 We present applications of the REWARE algorithm to two VHR sparker seismic profiles
157 acquired during two different surveys:

158 1) The METYSS 4 cruise (Gaullier & Watremez 2019) is dedicated to the architecture of
159 submarine canyons of the Eastern Sardinian continental shelf (Western Tyrrhenian, Italy);

160 2) The WATER cruise (Chanier & Gaullier 2017; Chanier & Watremez 2021) aims to
161 delineate the fault-systems in thick sedimentary basins in the shallow North Aegean Sea
162 (Greece).

163 The data used in these studies were acquired with a sparker source device. It generates
164 controlled seismic energy by creating a spark in the water, which vaporises the surrounding
165 water and creates a plasma bubble. The collapse of the bubble produces an acoustic wave
166 that propagate and reflect on the geological layers. In general, the frequency of a sparker
167 source ranges between 0.3 and 5 kHz, depending on the type of electrode, the energy level,
168 and the depth of tow. In the two case studies presented below, the frequency of the sparker
169 source ranges between 0.3 and 2 kHz.

170 After a correction of the acquisition geometry, each seismic profile is examined to look for
171 geological reflectors recorded in the water-column. The REWARE algorithm is used when
172 the water-column contains coherent signal, before applying a bandpass filter. For both
173 examples, we chose not to apply further common seismic processing workflows, such as

174 deconvolution, migration and gain recovery as these processes are time-consuming and the
175 resulting enhancement in signal quality does not justify the effort.

176 **4.1. Continental shelf crosscut by canyons**

177 During the METYSS 4 survey (Messinian Event in the Tyrrhenian from Seismic Study,
178 Gaullier & Watremez 2019) onboard the R/V Téthys II, more than 280 seismic profiles were
179 acquired along and across the Eastern Sardinian continental shelf of the hyper-extended
180 Western Tyrrhenian margin (Rehault *et al.* 1987; Jolivet & Faccenna 2000; Gaullier *et al.*
181 2014; Lymer *et al.* 2018). The acquisition system comprises one seismic source (sparker SIG
182 300 Joules), a digital single-channel streamer and the SonarWiz@6 acquisition software. The
183 great variability in bathymetry along the profiles required frequent changes in acquisition
184 parameters, particularly the shot spacing dictating the record length. Two sets of acquisition
185 parameters have been applied:

- 186 1) Mode 1: On the continental shelf at shallow water depths (c. 50–100 m): the shot
187 interval is 0.533 seconds (i.e., shot spacing of 1.1 m in using a ship speed of 4 knots).
188 The record length is 533 milliseconds (ms) TWTT with a sampling rate of 0.25 ms.
189 The energy output is 150 Joules for the sparker source. The vertical resolution is
190 approximately 0.6 m.
- 191 2) Mode 2: On the upper continental slope at deeper water depths (c. 600–1000 m), the
192 shot interval is 1 second (i.e., shot spacing of ~2.1 m in using a ship speed of 4
193 knots). The record length is 1 s with a sampling rate of 0.25 ms. The energy output is
194 300 Joules. The vertical resolution is around 1 m.

195 Some seismic profiles acquired in Mode 1 show heterogeneous bathymetry, as the area of
196 the canyon heads (Fig. 3d) reaches deeper water depth (c. 1000 m).

197 The selected seismic profile (Figure 3a) shows the Diedda Canyon along the Western
198 Sardinian platform (Fig. 3d). The acquisition parameters of this profile were set to Mode 1,
199 adapted to obtain a high spatial resolution for a maximum investigation depth of

200 approximately 400 m. The record length of 0.533 s does not show the thalweg of the canyon,
201 which occurs at ~800 ms TWTT (600 m water depth). However, an image of this geological
202 feature appears clearly in the water-column (Fig. 3a, shotpoints 5500–6500). The REWARE
203 algorithm (Fig. 3b) complements the infill reflectors in the canyon with an optimal vertical
204 resolution and trace-to-trace coherency. Various discontinuities in the Diedda canyon
205 (coloured lines on Fig. 3c), including the Messinian Erosion Surface (Lymer et al. 2018;
206 Sylvain et al. 2023), and separating several Plio-Quaternary sedimentary units (Fig. 3c) are
207 delineated thanks to the high vertical resolution of this dataset.

ORIGINAL UNEDITED MANUSCRIPT

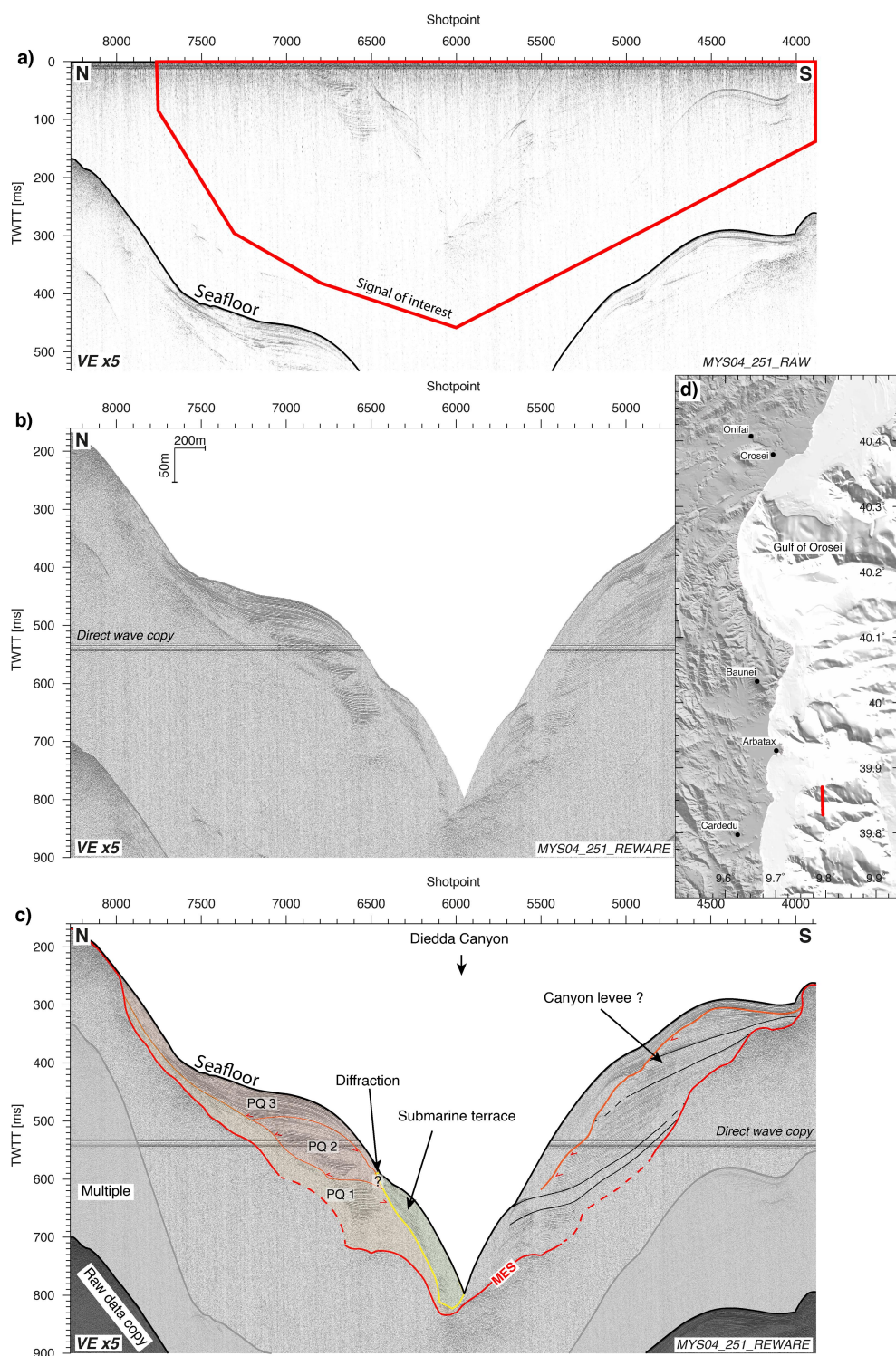


Figure 3. (a) Raw seismic section of the MYS04_251 profile illustrating the presence of coherent signal from previous shot recorded in the water-column. (b) Uninterpreted and (c) interpreted REWARE section of the MYS04_251 seismic profile (Sylvain et al. 2023). A

ORIGINAL

geometry correction, the REWARE algorithm, a bandpass filter and a water mute were applied. The restored part of the Diedda Canyon is under the “direct wave copy” between 533 and 800 ms TWTT. The red line corresponds to the Messinian Erosion Surface, the orange lines delineate the discontinuities limits between PQ 1, PQ 2 & PQ 3 units, and the yellow line highlights the discontinuity between PQ units and the submarine terrace (d) Location of the profile (red line), along the eastern Sardinia shelf. The map shading highlights the relief. Bathymetric data are extracted from the MAGIC project (Rosini & Cara 2021). Topographic data are extracted from the ALOS database (Tadono et al. 2014).

208

209 **4.2. Tectonically active rift basin**

210 The second example of data is a seismic profile acquired in the North Aegean Sea during the
211 WATER cruise (Western Aegean Tectonic Evolution and Reactivations; Chanier & Gaullier
212 2017; Chanier & Watremez 2021), which is dedicated to the study of fault patterns at the
213 junction of active rift basins and the western prolongation of the North Anatolian Fault (Caroir
214 et al. 2024). This area is mostly characterised by shallow water depths (30–60 m) locally
215 displaying very heterogeneous seafloor morphology, with steep slopes towards deep troughs
216 that can reach water depths down to 500 m. To obtain a VHR image of tectonic deformations
217 and associated sedimentary structures, the acquisition system and configuration were similar
218 to the ones used during the METYSS 4 cruise.

219 The great variability in bathymetry along the profiles would have required frequent changes
220 in acquisition parameters. However, a high trace-by-trace consistency was favoured by using
221 a short shot interval of 0.533 seconds (i.e., 1.1 m shot spacing at a vessel speed of 4 knots).
222 Therefore, the areas at water-depths >400 m. were neglected.

223 The selected seismic section from the WATER survey (Fig. 4) shows the benefits of applying
224 the REWARE algorithm to the seismic profile. The deeper seismic section has been restored,
225 highlighting thick faulted sedimentary sequences, while maintaining the high spatial
226 resolution. On the raw section (Fig. 4a), the seafloor is located between 350 and

227 410 ms TWTT (i.e., 262–307 m water depths). To keep the very high spatial resolution, the
228 record length was limited to 533 ms TWTT, allowing for only 150 ms TWTT of geological
229 record beneath the seafloor to be imaged. In addition, several normal faults are observed
230 with a limited vertical extension, and therefore their dip-directions remained relatively
231 unclear. The REWARE data extends the observations relative to the faults and the offsets of
232 the corresponding reflectors at depth, only by adding the reflections from previous shots
233 recorded in the water-column. For instance, on the REWARE data (Fig. 4c), the central fault
234 can be followed more than 200 ms TWTT longer than on the raw data (Fig. 4a). Not only the
235 faults, but also the architecture of the sedimentary deposits, are revealed thanks to the
236 integration of REWARE into the seismic processing workflow.

ORIGINAL UNEDITED MANUSCRIPT

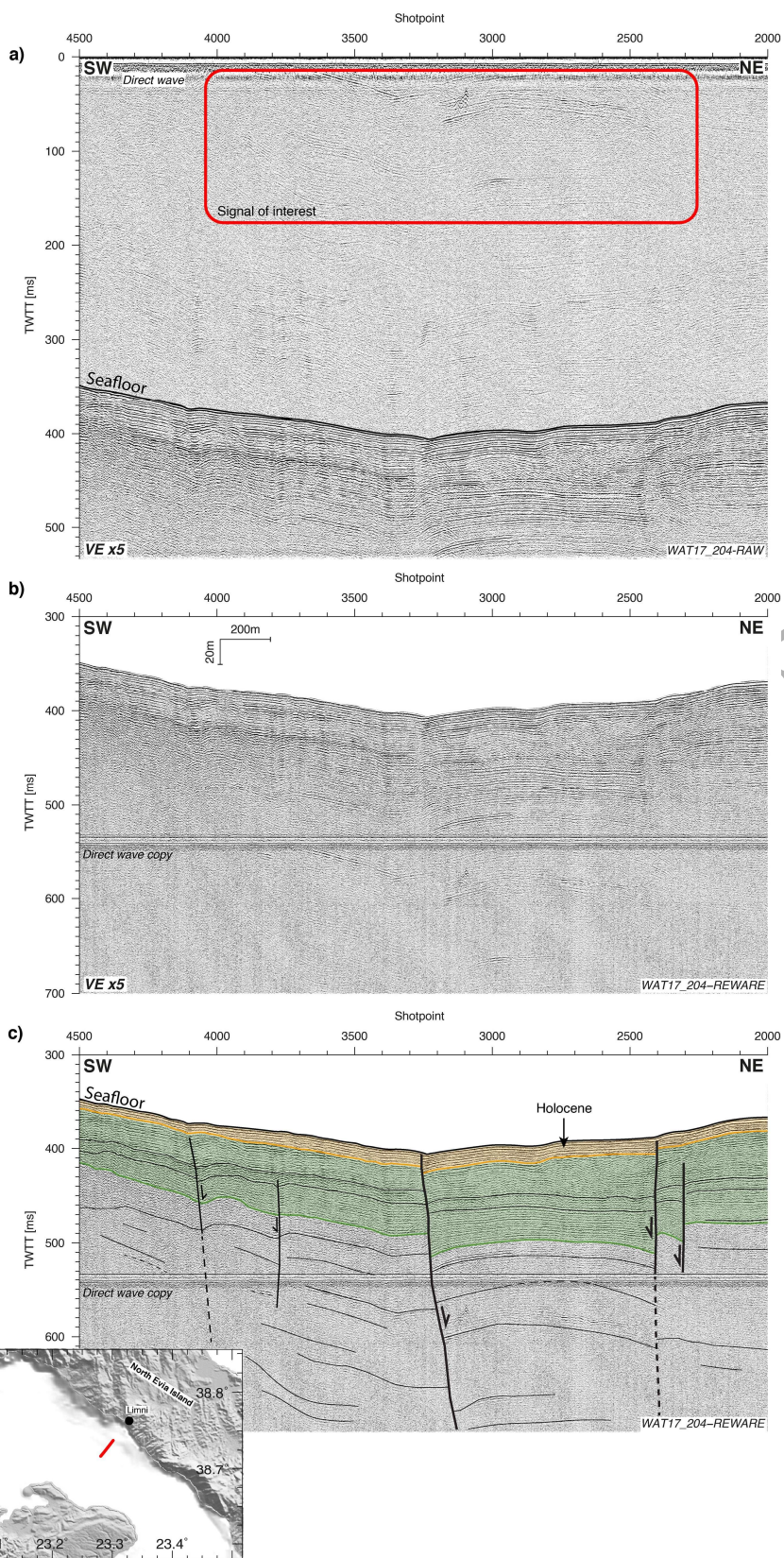


Figure 4. (a) Raw seismic section of the WAT17_204 profile illustrating the presence of

coherent signal from previous shot recorded in the water-column. (b) Uninterpreted and (c) interpreted REWARE section of the WAT17_204 seismic profile. A geometry correction, the REWARE algorithm, a bandpass filter and a water mute were applied. The seismic part added under the “direct wave copy”, between 533 and 700 ms TWTT, is the signal of the water-column. (d) Location map of the seismic section (red line), south of North Evia Island. Bathymetric and topographic data are extracted from GMRT (Ryan et al. 2009)

237

238 **5. Discussion**

239 Here we discuss how to best combine REWARE with other standard steps of single-channel
240 seismic processing, such as filtering, deconvolution, migration, and static correction (Yilmaz
241 & Doherty 2001; Dondurur 2018; Santos et al. 2021).

242 When REWARE is applied first in the processing workflow, the occurrence of the copy of the
243 direct wave in the middle of the section has consequences on further processing. (1) A
244 migration in the T-K domain may be applied on this single-channel dataset (equivalent to a
245 2D post-stack migration with constant velocity; Stockwell 1999). However, the copy of the
246 direct wave causes over-migration (“smile”) artefacts (Dondurur 2018), which will corrupt the
247 reflectors above this event. Please note it is also important to check for the presence of
248 random spikes (electronic noise) that may also happen with sparker data, also leading to
249 over-migration artefacts. Thus, the migration should be applied prior to the REWARE
250 algorithm, and on data showing no random spikes. (2) Some algorithms for gain recovery are
251 affected by REWARE. An automatic gain control (AGC) is not recommended with REWARE
252 due to the high amplitude of the direct wave. Indeed, the AGC will lower the amplitude above
253 the seabed but also above the direct wave copy, resulting in a quiet zone affecting the
254 reflectors. (3) Another gain recovery algorithm, such as the spherical divergence correction,
255 corrects the loss of amplitude of the acoustic wave due to the increasing distance from the
256 source. The amplitude of late arrivals becomes more visible with this correction, which does

257 not affect the relative amplitude variations at depth (Dondurur 2018). A spherical divergence
258 spreading correction (Yilmaz & Doherty 2001) has been tested before REWARE, but it
259 decreases the amplitudes of the coherent signal in the water-column, which is incompatible
260 with the purpose of the REWARE processing algorithm. However, using the spherical
261 divergence spreading correction after applying the REWARE algorithm will increase the
262 amplitude of the late arrivals without modifying seismic facies. (4) A deconvolution may be
263 applied to a dataset. For air-gun data, the deconvolution is well known and easy to apply as
264 the wave source is the same for each trace. However, for sparker data, the deconvolution is
265 complex and time-consuming as the wave source is different from one shot to another
266 (Duchesne *et al.* 2007). A single operator can be used along an entire profile, although this is
267 not optimal for sparker data. This solution works best for airgun data. The deconvolution may
268 be applied on the data either before the REWARE algorithm, or after. Static corrections
269 include suppression of the action of tides and waves affecting the sea surface (Lacombe *et*
270 *al.* 2009; Kim *et al.* 2017).

271 We propose a processing workflow for single-channel data (Fig 5), modified from Santos *et*
272 *al.* (2021). This processing workflow implements the REWARE algorithm and allows to use
273 common processing tools, such as deconvolution, migration, gain recovery or filtering, to
274 their full potential.

275 In summary, the seismic processing workflow proposed follows:

- 276 (1) Geometry correction,
- 277 (2) Filtering (e.g. bandpass filter, F-K filter, etc.),
- 278 (3) Deconvolution,
- 279 (4) Static corrections,
- 280 (5) Migration,
- 281 (6) REWARE,
- 282 (7) Spherical Divergence Correction,
- 283 (8) Water mute (amplitudes are set to zero above the seafloor).

284 **6. Conclusion**

285 REWARE is a very simple and rapid method using the late arrivals from the previous shot
286 recorded in the water-column to obtain further geological information. This method can be
287 applied to marine Very-High-Resolution single-channel seismic reflection profiles. The
288 REWARE algorithm is an open-source code provided as a Shell script and using Seismic
289 Un*x modules (Supplementary materials) to integrate in the seismic processing workflow. For
290 each seismic trace, it retrieves the coherent signal from the previous shot, recorded in the
291 water-column, and add it at the end of previous traces, artificially extending the record length.
292 This processing allows to optimise the acquired marine VHR seismic data. Moreover, this
293 method solves the conflict between the need to obtain more information at depth below the
294 seafloor (long record length) and maintaining an initial high spatial resolution (high source
295 frequency and short shot interval).

296 From two case studies, we demonstrate that the coherent signal recorded in the water-
297 column of the seismic section may be retrieved and can provide useful information on the
298 geological structures beneath the seafloor. We show the potential of this processing for
299 sedimentology or structural geology studies at variable water depths, on the continental
300 shelves and associated slopes and canyons, while maintaining good resolution of
301 sedimentary sequences, unconformities, and tectonic features.

302 In offshore areas, with low to moderate bathymetry and especially with high morphological
303 variability, this processing limits the need to changes in acquisition parameters each time
304 bathymetry varies, thus optimising acquisition times. The approach minimizes seismic gaps
305 where water-depth increases, without additional acquisition time.

306

307

308

309 **Acknowledgements**

310 We are grateful to the Captains of the R/V 'Téthys II' Dany Deneuve (METYSS 4), Joël
311 Perrot (WATER 1), Arnaud Behoteguy (WATER 2), their crews and all the scientific members
312 onboard for data acquisition during 'METYSS 4' and 'WATER 1 & 2' cruises. Maps and
313 seismic profiles were realised with the Generic Mapping Tools software (Wessel et al. 2013).
314 All the development of this method is based on the Seismic Un*x package (Stockwell 1999;
315 Cohen & Stockwell 2021). The 'METYSS 4' and 'WATER 1 and 2' cruises were supported by
316 FMAFC (Fond Mutualisé d'Accompagnement Financier des Campagnes) and by the TelluS
317 program of CNRS-INSU, "Post-Campagnes à la mer". The sparker equipment was funded by
318 the European Union (ERDF), the French State, the French Region Hauts-de-France and
319 Ifremer in the framework of the project CPER MARCO 2015-2021. We also thank the two
320 anonymous reviewer's constructive comments, which greatly helped improve the quality of
321 this manuscript.

322 **Author Contribution**

323 Romain Sylvain: Writing – original draft; Writing – review & editing; Visualization;
324 Methodology

325 Louise Watremez: Writing – original draft; Writing – review & editing; Methodology;
326 Supervision; Data acquisition

327 Isabelle Thinon: Writing – review & editing; Methodology; Data acquisition

328 Frank Chanier: Writing – review & editing; Supervision; Data acquisition

329 Fabien Caroïr: Writing – review & editing; Visualization; Data acquisition

330 Virginie Gaullier: Writing – review & editing; Supervision; Data acquisition

331

332

333 **Data Availability Statement**

334 The data underlying this article are available in the article and in its online supplementary
335 material.

336

337 **References**

338 Bakhtiari Rad, P. & Macelloni, L., 2020. Improving 3D water column seismic imaging using
339 the Common Reflection Surface method. *Journal of Applied Geophysics*, **179**,
340 104072. doi:10.1016/j.jappgeo.2020.104072

341 Caroir, F., Chanier, F., Gaullier, V., Sakellariou, D., Bailleul, J., Maillard, A., Paquet, F., *et al.*,
342 2024. Late Quaternary deformation in the western extension of the North Anatolian
343 Fault (North Evia, Greece): Insights from very high-resolution seismic data (WATER
344 surveys). *Tectonophysics*, **870**, 230138. doi:10.1016/j.tecto.2023.230138

345 Chanier, F. & Gaullier, V., 2017. WATER cruise, Téthys II R/V, Sismar.
346 doi:10.17600/17009400

347 Chanier, F. & Watremez, L., 2021. WATER 2 cruise, Téthys II R/V, Sismar.
348 doi:10.17600/18001115

349 Cohen, J.K. & Stockwell, J.W., 2021. CWP/SU: Seismic Un*x Release No. 44R22: an open
350 source software package for seismic research and processing. *Center for Wave*
351 *Phenomena, Colorado School of Mines.*

352 Dondurur, D., 2018. *Acquisition and processing of marine seismic data*, Elsevier.

353 Duchesne, M.J., Bellefleur, G., Galbraith, M., Kolesar, R. & Kuzmiski, R., 2007. Strategies for
354 waveform processing in sparker data. *Mar Geophys Res*, **28**, 153–164.
355 doi:10.1007/s11001-007-9023-8

356 Gaullier, V., Chanier, F., Lymer, G., Vendeville, B.C., Maillard, A., Thion, I., Lofi, J., *et al.*,
357 2014. Salt tectonics and crustal tectonics along the Eastern Sardinian margin,

358 Western Tyrrhenian: New insights from the “METYSS 1” cruise. *Tectonophysics*,
359 **615–616**, 69–84. doi:10.1016/j.tecto.2013.12.015

360 Gaullier, V. & Watremez, L., 2019. METYSS 4 cruise, Téthys II R/V, Sismar.
361 doi:10.17600/18001156

362 Jolivet, L. & Faccenna, C., 2000. Mediterranean extension and the Africa-Eurasia collision.
363 *Tectonics*, **19**, 1095–1106. doi:10.1029/2000TC900018

364 Jun, H., Jou, H.-T., Kim, C.-H., Lee, S.H. & Kim, H.-J., 2020. Random noise attenuation of
365 sparker seismic oceanography data with machine learning. *Ocean Sci.*, **16**, 1367–
366 1383. doi:10.5194/os-16-1367-2020

367 Kim, H., Lee, G.H., Yi, B.Y., Yoon, Y., Kim, K.-O., Kim, H.-J. & Lee, S.H., 2017. A simple
368 method of correction for profile-length water-column height variations in high-
369 resolution, shallow-water seismic data. *Ocean Sci. J.*, **52**, 283–292.
370 doi:10.1007/s12601-017-0019-2

371 Kluesner, J., Brothers, D., Hart, P., Miller, N. & Hatcher, G., 2019. Practical approaches to
372 maximizing the resolution of sparker seismic reflection data. *Mar Geophys Res*, **40**,
373 279–301. doi:10.1007/s11001-018-9367-2

374 Lacombe, C., Butt, S., Mackenzie, G., Schons, M. & Bornard, R., 2009. Correcting for water-
375 column variations. *The Leading Edge*, **28**, 198–201. doi:10.1190/1.3086058

376 Lymer, G., Lofi, J., Gaullier, V., Maillard, A., Thinon, I., Sage, F., Chanier, F., *et al.*, 2018.
377 The Western Tyrrhenian Sea revisited: New evidence for a rifted basin during the
378 Messinian Salinity Crisis. *Marine Geology*, **398**, 1–21.
379 doi:10.1016/j.margeo.2017.12.009

380 Rehault, J.-P., Mascle, J., Fabbri, A., Moussat, E. & Thommeret, M., 1987. The Tyrrhenian
381 Sea before Leg 107. *Proceedings of the Ocean Drilling Program, Initial Reports*, **107**,
382 9–35. doi:10.2973/odp.proc.ir.107.102.1987

383 Rosini, U. & Cara, P., 2021, September 23. MAGIC Progetto. Retrieved from
384 <https://github.com/pcm-dpc/MaGIC>

- 385 Ruddick, B., Song, H., Dong, C. & Pinheiro, L., 2009. Water Column Seismic Images as
386 Maps of Temperature Gradient. *Oceanog.*, **22**, 192–205.
387 doi:10.5670/oceanog.2009.19
- 388 Ryan, W.B.F., Carbotte, S.M., Coplan, J.O., O'Hara, S., Melkonian, A., Arko, R., Weissel,
389 R.A., *et al.*, 2009. Global Multi-Resolution Topography synthesis: GLOBAL MULTI-
390 RESOLUTION TOPOGRAPHY SYNTHESIS. *Geochem. Geophys. Geosyst.*, **10**, n/a-
391 n/a. doi:10.1029/2008GC002332
- 392 Santos, I.D., Gomes, M.P., Garabito, G., Vital, H. & Lopes, V.H.R., 2021. High-Resolution
393 Marine Seismic Data Processing Using a Single-Channel Sparker System: Bahia
394 Shelf, Brazil. *Braz J Geophys*, **39**, 209. doi:10.22564/rbgf.v39i3.2095
- 395 Sliter, R.W., Triezenberg, P.J. & Hart, P.E., 2008. High-Resolution Chirp and Mini-Sparker
396 Seismic-reflection Data From the Southern California Continental Shelf--Gaviota to
397 Mugu Canyon, U.S. Geological Survey Open-File Report 2008-1246, . Retrieved from
398 <https://pubs.usgs.gov/of/2008/1246/>
- 399 Stockwell, J.W., 1999. The CWP/SU: Seismic Un*x package. *Computers & Geosciences*, **25**,
400 415–419. doi:10.1016/S0098-3004(98)00145-9
- 401 Sylvain, R., Gaullier, V., Watremez, L., Chanier, F., Caroir, F., Graveleau, F., Lofi, J., *et al.*,
402 2023. The Messinian Erosion Surface along the Eastern Sardinian Margin, Western
403 Tyrrhenian: New Insights from Very High-Resolution Seismic Data (METYSS 4)
404 (Poster No. EGU23-13909), Vienna: EGU23. doi:10.5194/egusphere-egu23-13909
- 405 Tadono, T., Ishida, H., Oda, F., Naito, S., Minakawa, K. & Iwamoto, H., 2014. Precise Global
406 DEM Generation by ALOS PRISM. *ISPRS Ann. Photogramm. Remote Sens. Spatial*
407 *Inf. Sci.*, **II-4**, 71–76. doi:10.5194/isprsannals-II-4-71-2014
- 408 Wessel, P., Smith, W.H.F., Scharroo, R., Luis, J. & Wobbe, F., 2013. Generic Mapping
409 Tools: Improved Version Released. *Eos Trans. AGU*, **94**, 409–410.
410 doi:10.1002/2013EO450001

411 Yilmaz, Ö. & Doherty, S.M., 2001. *Seismic data analysis: processing, inversion, and*
412 *interpretation of seismic data*. Investigations in geophysics, 2nd ed., Vols 1-2, Vol. 1,
413 Society of Exploration Geophysicists.
414

ORIGINAL UNEDITED MANUSCRIPT